Article ID: 1003 - 6326(2004)06 - 1162 - 07

Structure and tensile/ wear properties of microarc oxidation ceramic coatings on aluminium alloy①

WEI Tong-bo(魏同波), YAN Feng-yuan(阎逢元), LIU Wei-min(刘维民), TIAN Jun(田 军)
(State Key Laboratory of Solid Lubrication, Lanzhou Institute of Chemical Physics, Chinese Academy of Sciences, Lanzhou 730000, China)

Abstract: Thick and hard ceramic coatings were prepared on the Al-Cu-Mg alloy by microarc oxidation in alkali-silicate electrolytic solution. The thickness and microhardness of the oxide coatings were measured. The influence of current density on the growth rate of the coating was examined. The microstructure and phase composition of the coatings were investigated by means of scanning electron microscopy, energy dispersive spectroscopy, and X-ray diffraction. Moreover, the tensile strength of the Al alloy before and after microarc oxidation treatment were tested, and the fractography and morphology of the oxide coatings were observed using scanning electron microscope. It is found that the current density considerably influences the growth rate of the microarc oxidation coatings. The oxide coating is mainly composed of α-Al_2O_3 and γ-Al_2O_3, while high content of Si is observed in the superficial layer of the coating. The cross-section microhardness of 120 μm thick coating reaches the maximum at distance of 35 μm from the substrate/ coating interface. The tensile strength and elongation of the coated Al alloy significantly decrease with increasing coating thickness. The microarc oxidation coatings greatly improve the wear resistance of Al alloy, but have high friction coefficient which changes in the range of 0.7 - 0.8. Under grease lubricating, friction coefficient is only 0.15 and wear loss is less than 1/ 10 of the loss under dry friction.

Key words: microarc oxidation; ceramic coatings; aluminium alloys
CLC number: TG 174.453 **Document code:** A

1 INTRODUCTION

Aluminium and its alloys have found wide application in engineering, owing to their good specific strength and light mass. However, a poor surface hardness and a relatively low yield strength of aluminium alloys make these materials vulnerable to wear in high load situations, which limits their practical use. Microarc oxidation (MAO), also called plasma electrolytic oxidation (PEO), is a novel technique developed to produce hard ceramic coatings on valve metals such as Al, Ti, Mg and their alloys[1-4], which is characterized by a high temperature of 10^3 - 10^4 K and a high local pressure of 10^2 - 10^3 MPa in discharge channels[5]. With the introduction of hard ceramic coatings by means of microarc oxidation, wear resistance, corrosion resistance, mechanical strength, and electrical insulation of metals and their alloys can be effectively increased[6-12]. This is especially true for Al and its alloys, which is imperative to extend the application fields of Al alloys in aerospace, automotive, and textile engineering, etc[13, 14]. However, the effect of microarc oxidation on the mechanical properties of Al alloys has not been well explored, which is critical to the practical use of Al alloys subjected to microarc oxidation treatment. With this perspective in mind, thick oxide coatings were fabricated on Al alloys by the MAO process. The influence of current density on the growth rate of the oxide coating was studied. The microstructure, phase composition, and mechanical properties of oxide coatings were analysed, with an emphasis placed on the effect of the MAO treatment on the tensile and antiwear properties of the alloy.

2 EXPERIMENTAL

Sheets of 100 mm × 40 mm × 1.5 mm made of LY12 Al alloy (0.50% Si and Fe, 3.8% - 4.9% Cu, 0.30% - 0.90% Mn, 1.20% - 1.80% Mg, 0.30% Zn, balance Al) were ground to an average surface roughness R_a= (1.2 ±0.3) μm, cleaned with a detergent and then washed with distilled water before subjecting to the oxidation process. Ceramic coatings were prepared with a 20 kW microarc oxidation equipment consisting of a potential adjustable pulsed DC source, a stainless steel container with a sample-holder as an electrolyte cell, stirring and cooling systems. An Al alloy specimen and the wall of a stainless steel container were used as anode and cathode, respectively. The electrolytic

① **Foundation item:** Project (50271080) supported by the National Natural Science Foundation of China
Received date: 2003 - 12 - 02; **Accepted date:** 2004 - 08 - 01
Correspondence: YAN Feng-yuan, Professor, PhD; Tel: + 86-931-4968185; Fax: + 86-931-8277088; E-mail: fyyan@lzb.ac.cn

solution was composed of KOH and Na_2SiO_3 in distilled water. The solution temperature was kept below 35 ℃ during oxidation. Predefined current density on the specimen surface was maintained by controlling the voltage within 400 – 600 V and the ratio of the cathodic (I_c) to anodic (I_a) currents is $I_c/I_a = 1$, namely $I = I_c = I_a$. The coatings of different thickness were obtained by controlling the treatment time.

The thickness of the oxide coatings was measured with a MINITEST 1100 microprocessor coating thickness gauge (Elektro-physik Koln) based on the eddy current technique before and after the loose layer of the coating was removed. The morphology of the oxide coatings were observed with a JSM-5600LV scanning electron microscope (SEM). The elemental composition of the oxide coating was determined using an X-ray energy dispersive spectrometer (EDS) attached to the scanning electron microscope. The crystallographic characteristics of the microarc coatings were investigated on a Siemens D5000 X-ray diffractometer, using Cu K_α radiation. After the oxide coatings were polished with SiC paper to remove the loose layer, the surface hardness of the dense layers was measured using a Mitutoyo MVK G1 microhardness tester with a Vickers indenter, at a load of 1 N. The cross-section hardness of the coatings was also measured in the same manner.

The coated specimens were cut into slabs of 80 mm × 10 mm × 1.5 mm for tensile tests. The tensile strengths of the specimens were evaluated at a drawing velocity of 0.05 mm/s using an MTS-810 machine which automatically recorded the stress-strain curves. The 60 μm thick oxidation coatings were abraded with SiC paper to remove the outer loose layer about 20 μm thick and evaluated on an THT07-135 ball-on-disk friction and wear tester under both dry- and grease-lubricated conditions, using d3 mm Si_3N_4 ceramic ball and GCr15 ball as the counterparts. The load and sliding speed was 10 N and 0.2 m/s, respectively. Diameter of wear track on disk was 12 mm. The wear rate of oxidation coatings was determined by measuring the wear scar cross-sectional area with a BCJ-2 profilometer and the wear loss of balls was calculated by measuring the wear scar diameter with microscope. The wear loss of alloys was measured by 328A scale. The morphology and fractography of the oxide coatings subjected to tensile and friction tests were investigated by means of SEM.

3 RESULTS AND DISCUSSION

3.1 Effect of current density on growth rate of microarc oxidation coatings

Fig. 1(a) shows the variation of thickness of the as-deposited coating with the microarc oxidation treatment time. It is seen that the thickness of the coating increases linearly with time and the linear rate constant equals to the hourly coating thickness. It is also seen that the current density greatly influences the growth rate of oxide coatings. Fig. 1(b) shows the variation of the dense layer thickness with the microarc oxidation treatment time. A similar changing tendency of the dense layer thickness with the treatment time is also observed in this case. Nevertheless, at the same time, as the current density exceeds 6.0 A/dm^2, its influence on the growth rate of the dense layer decreases significantly. Ultimately, the growth rate of the dense layer will remain constant with increasing current density. It is also seen that when current density increases, the ratio of dense layer to total coating diminishes from Fig. 1(a) and Fig. 1(b). The results are different from what Xue et al[15] had obtained.

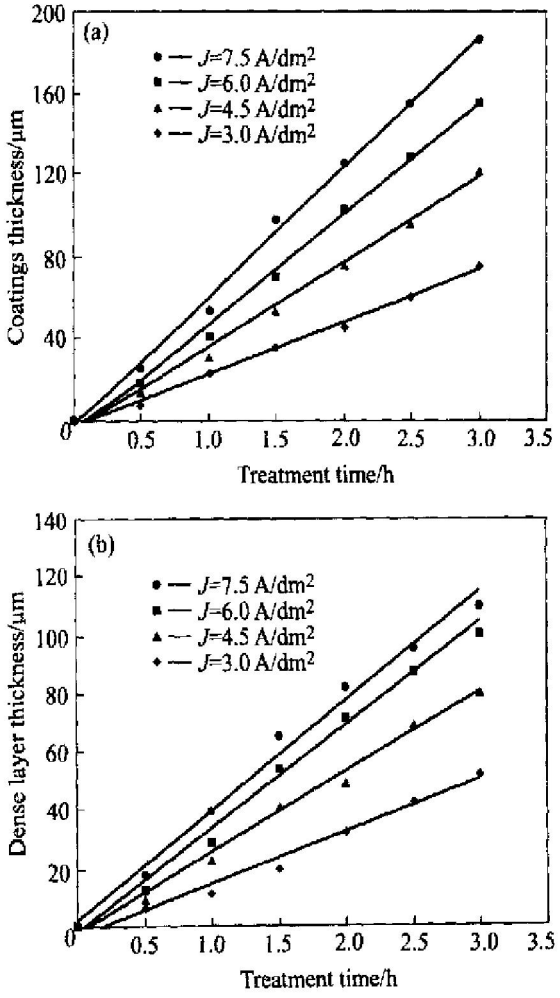

Fig. 1 Variation of thickness of as-deposited coating (a) and dense layer (b) with MAO treatment time at different current densities

3.2 Element and phase composition of microarc oxidation coatings

The EDS spectra collected from the cross-section of the coating show that the loose layer is composed of Al, Si and O, and Si exists in the loose layer at mass fraction of 20% – 40%, while the dense layer is mainly composed of

Al and O. The growth of oxide coating mainly depends on the combination between Al and O in microarc oxidation process. SiO_3^{2-} can enter into the outer layer of oxide coating by diffusion and electrophoresis etc. However, it can not enter into the inner layer due to the obstacle of melted alumina oxide, so Si is only found in loose layer. The phase distribution of the oxide coatings with XRD analysis is shown in Fig. 3. It is found that both the loose outlayer and the dense layer are mainly composed of α-Al_2O_3 and γ-Al_2O_3. The Al-Si-O phase ($Al_6Si_2O_{13}$) is found only in the loose layer. The α-Al_2O_3 content in the dense layer is higher than that in the loose layer. This is mainly caused by a variation in the cooling rate of the molten alumina in the microarc zone. In other words, the outer layer surface directly connected with the solution has a higher cooling rate to favor the formation of γ-Al_2O_3 phase during the solidification of alumina; while the inner layer retains higher temperature which is high enough to transform the newly-formed γ-Al_2O_3 to α-Al_2O_3, owing to low thermal conductivity of the alumina oxide. Thus, a considerably increased wear resistance of Al and its alloys after microarc oxidation treatment could be attributed to the formation of hard ceramic coatings.

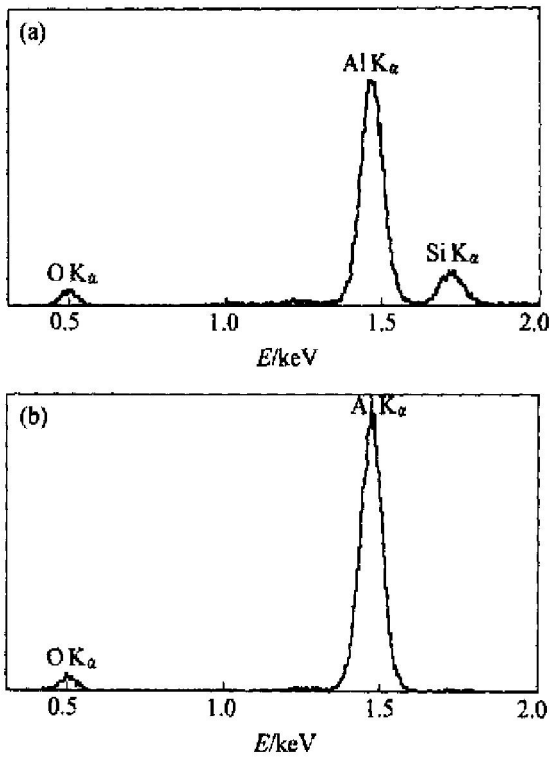

Fig. 2 EDAX spectra of loose layer(a) and dense layer(b) in microarc oxidation coating

3.3 Surface and cross-section microhardness of microarc oxidation coatings

The MAO coating obtained at a typical current density were polished to remove the loose layer, then the

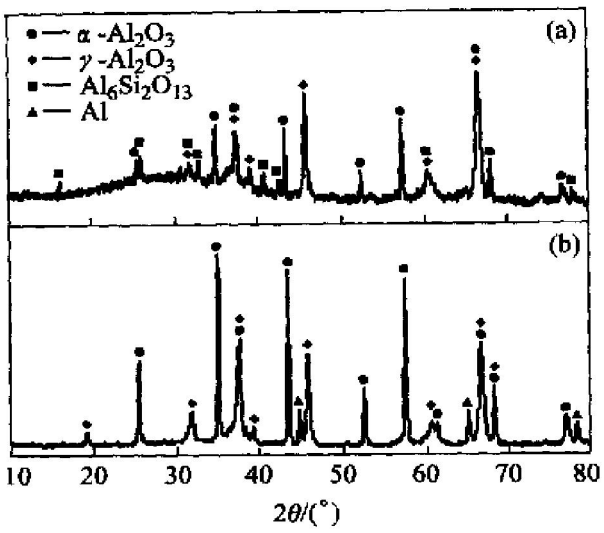

Fig. 3 XRD patterns of 120 μm-thick oxidation coating surface before polished (a) and after 40% polished (b)

hardness of the dense layer was measured. As shown in Fig. 4, the polished dense coating register hardness is even above 1 200$HV_{0.1}$, which increases gradually with the increasing coating thickness. The change has much with the phase composition of oxide coating. When the oxide coating thickness increases, the phase change in dense layer has reinforced and the content of α-Al_2O_3 increases, so the hardness of dense layer surface becomes larger with its increasing thickness. Fig. 5 shows the microhardness depth profile of the coatings. It is seen that the cross-section microhardness of the 120 μm coatings comes to the maximum of 1 600HV at a distance of 35 μm from the coating-substrate interface. This might be attributed to the changes in the phase composition and porosity of the coatings along the depth. As a matter of fact, the hardness and α-Al_2O_3 contents of the coatings show similar profiles[16], i. e., the maximal α-Al_2O_3 content corresponds to the maximal hardness. In other words, an increase in the contents of γ-Al_2O_3 and Si towards the coating surface leads to a decrease in hardness. No brittle cracking was observed on the coatings subjected to Vickers hardness indentation, which indicates that the coatings has good cohesive strength and toughness.

3.4 Tensile strength and elongation of coated aluminium alloys

Fig. 6 shows the tensile strengths (σ) and elongations (δ) of coated Al alloy with different coatings thicknesses. It can be seen that the tensile strength slightly decreases with the increasing coating thickness, however, the elongation first decreases rapidly and then gradually decreases with the increasing coating thickness, which

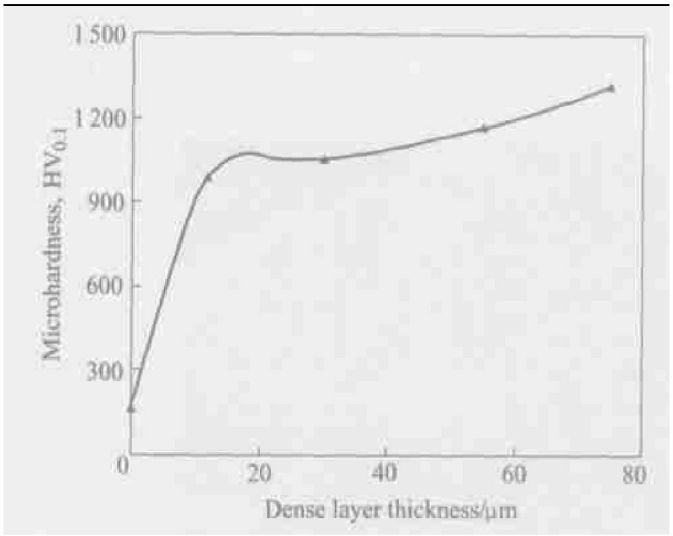

Fig. 4 Variation of hardness of dense layer with coating thickness

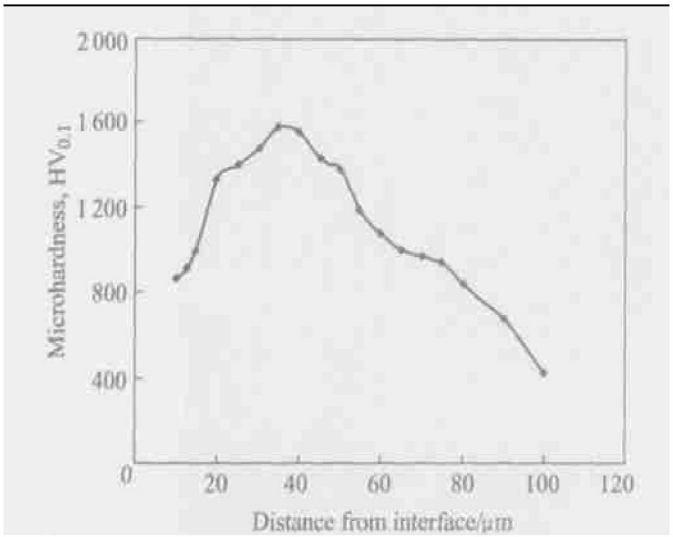

Fig. 5 Variation in cross-section microhardness of oxide coating with distance from substrate/coating interface

suggests that the rigidity of the coated Al alloy is strengthened. This is caused by the character difference between metal and ceramic oxide coating. Their distortion is not concurrent in tensile process. The thicker the oxide coating is, the more brittle it will be, and hence it has stronger anchoring effect on Al alloy which has high toughness and tensile strength, thus weakeness the tensile strength of the coated alloys. In the tensile strength test it was observed that the ceramic coatings of 60 μm and 130 μm have not been stripped from the alloy substrate on a large area and a large number of cracks appeared on the coating surface, as shown in Fig. 7. Furthermore, the thinner coating shows cracks of relatively smaller size. However, the 165 μm oxidation coatings have been stripped on a large area. The fractographs of the oxide coatings of 60 μm and 130 μm indicate that the oxide coatings are not stripped and cracks of larger size occur about 20 – 50 μm from the coating/substrate interface (Figs. 7(e) and (f)). This demonstrates that the MAO coatings have excellent adhesion with the Al alloy substrate. It was supposed that the good adhesion between the MAO coatings and the Al alloy substrate could be closely related to the metallurgical intermixing and interdiffusional bonding occurring at high temperature and pressure in the spark discharge process. Furthermore, the similar lattice structure of Al and γ-Al_2O_3 contributes to increase the interface interaction, while the micropores produced by microarc discharge may function to eliminate the residual stress. In addition, the hardness gradient near the coating/alloy also helps to eliminate the inherent stress. Therefore, the tensile strength of the coated Al alloy is retained owing to the good cohesion and toughness of oxide coatings. This is very advantageous for practical application of the microarc oxidation technique.

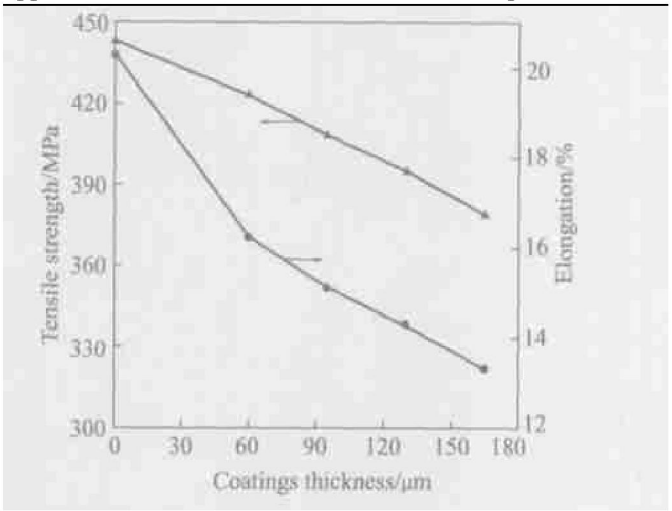

Fig. 6 Variation in tensile strength and elongation of coated Al alloys with coating thickness

3.5 Friction and wear behaviors

Variation of the friction coefficient with the sliding distance for microarc oxidation coatings under different friction conditions and against different counterparts is shown in Fig. 8. The friction coefficients against both Si_3N_4 ceramic ball and GCr15 ball under dry friction condition are higher and the former is relatively higher than the latter. The friction coefficient against Si_3N_4 ceramic ball is steady and almost 0.8, while the friction coefficient against GCr15 ball increases gradually and then keeps 0.73 after the sliding distance of 500 m. The phenomenon is resulted in by the high wear loss of GCr15 ball. Worn surface of MAO coatings against Si_3N_4 ceramic ball is shown in Figs. 9(a) and (b). It is seen that the larger cracks appear on the worn surface of oxidation coatings, so the primary wear mechanism of oxidation coatings

against ceramic ball is surface fracture. The surface of ceramic ball has wear particles (Fig. 9(c)) and the wear mechanism of ceramic ball is mostly slight grain wear and oxidation wear due to the friction heat. The wear loss of oxide coatings against GCr15 ball is less than 1/10 of the loss against ceramic ball because of its high hardness, as shown in Table 1. The primary wear mechanism of oxidation coatings against GCr15 ball is also surface fracture.

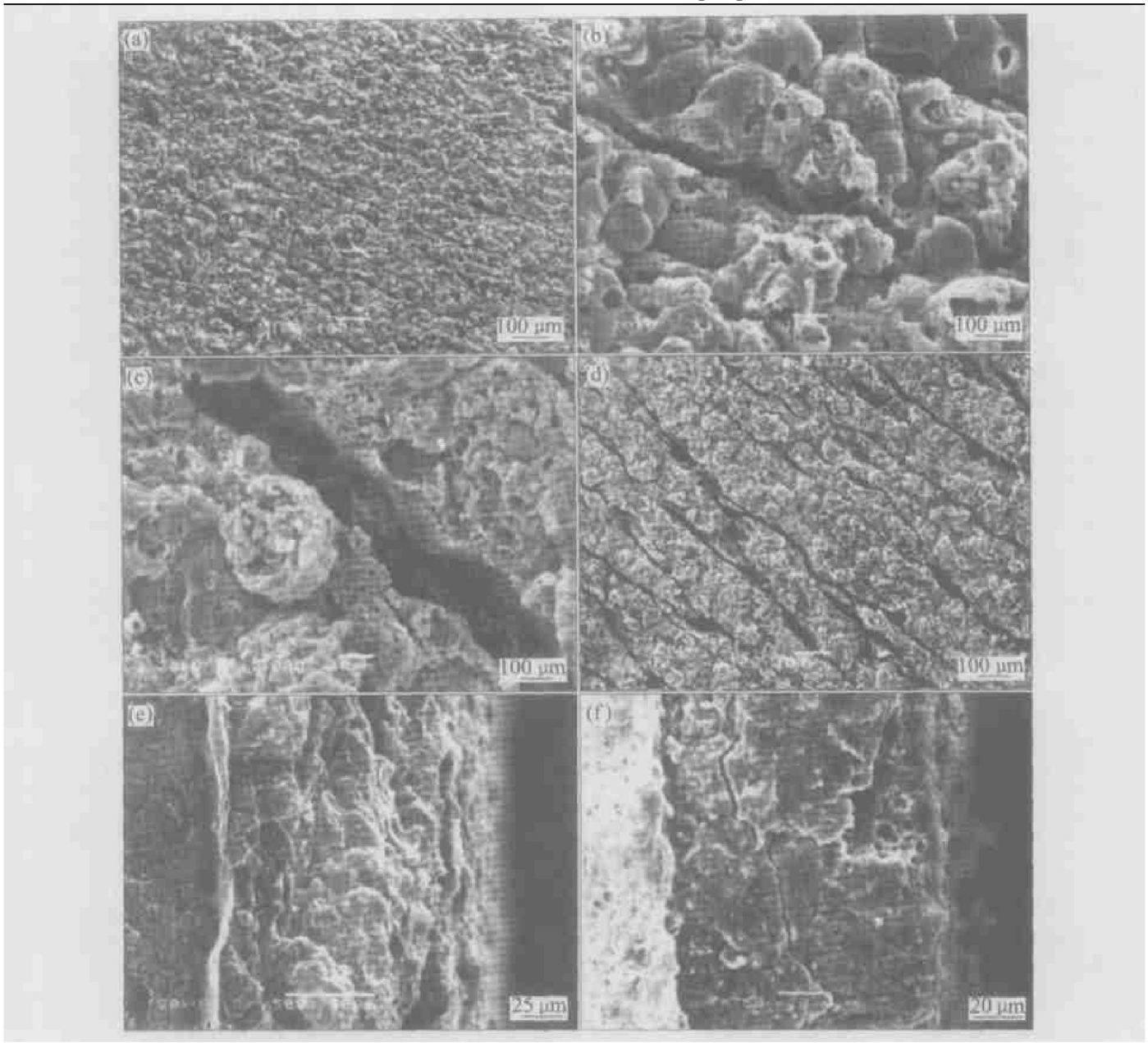

Fig. 7 Surface morphologies and fractographies of oxide coatings on Al alloy after tensile strength test
(a) —Surface morphology of 60 μm thick specimen; (c) —Surface morphology of 130 μm thick specimen; (b), (d) —Magnified images of (a) and (c); (e) —Fractography of 60 μm thick specimen; (f) —Fractography of 130 μm thick specimen

Table 1 Friction and wear test results of MAO coatings

Specimen	Counterpart	Friction condition	Distance/m	Friction coefficient	Specimen wear rate/($mm^3 \cdot N^{-1} \cdot m^{-1}$)	Counterpart wear rate/($mm^3 \cdot N^{-1} \cdot m^{-1}$)
Al	Si_3N_4 ball	Dry friction	100	0.85 - 0.44	2.0×10^{-3}	
Al	GCr15 ball	Dry friction	100	0.89 - 0.51	2.4×10^{-3}	
MAO coating	Si_3N_4 ball	Dry friction	1 000	0.78	4.2×10^{-5}	8.7×10^{-6}
MAO coating	Si_3N_4 ball	Grease lubricating	1 000	0.15	1.4×10^{-6}	1.8×10^{-7}
MAO coating	GCr15 ball	Dry friction	1 000	0.71	1.1×10^{-6}	3.0×10^{-5}
MAO coating	GCr15 ball	Grease lubricating	1 000	0.14		4.1×10^{-6}

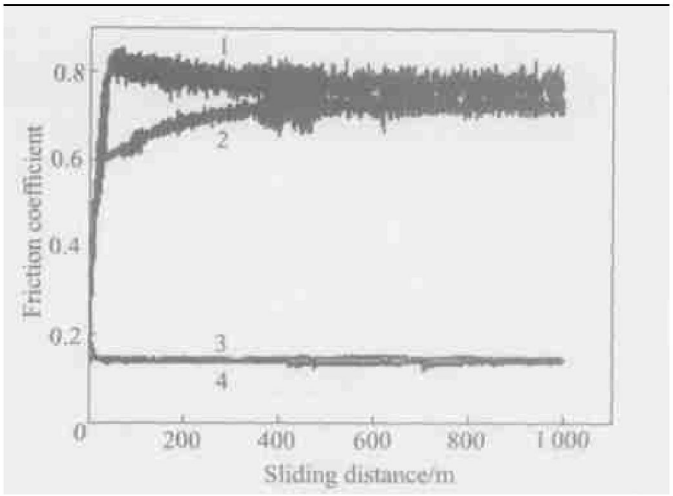

Fig. 8 Variation of friction coefficient with sliding distance in ball-on-disk sliding tests of MAO coatings
1 —Si_3N_4 ceramic ball under dry friction;
2 —GCr15 ball under dry friction;
3 —Si_3N_4 ceramic ball under grease lubricating;
4 —GCr15 ball under grease lubricating

The slight grooves appear on the worn surface of GCr15 ball in Fig. 9 (d) and its primary wear mechanism is slight plastic deformation. The friction coefficient is only 0.15 against two counterparts under FLZ-3 lubricating grease. Both the oxide coatings and the counterparts have less wear loss, which is less than 1/10 of the loss under dry friction. The friction coefficient against the Al alloys is initially high, but then becomes significantly reduced, from 0.85 to 0.44 for Si_3N_4 ceramic ball and from 0.89 to 0.51 for GCr15 ball, respectively. The reduction is contributed to by increasing oxidation of the aluminium, which transforms the friction/wear mechanism.

4 CONCLUSIONS

The thickness of the microarc oxidation coatings on Al alloy increases linearly with increasing treatment duration and is largely dependent on the applied current density. The microarc oxidation coatings are divided into the loose superficial layer and the inner dense layer and they are mainly composed of α-Al_2O_3 and γ-Al_2O_3, while high content of Si is observed in the superficial layer of the coating. The cross-section microhardness has the maximum at a distance of 35 μm from the interface, then it decreases with increasing distance from the interface. The surface hardness of the dense layer increases with increasing coating thickness, while the tensile strength and elongation decrease with increasing coating thickness. After the tensile tests are completed, many cracks are produced

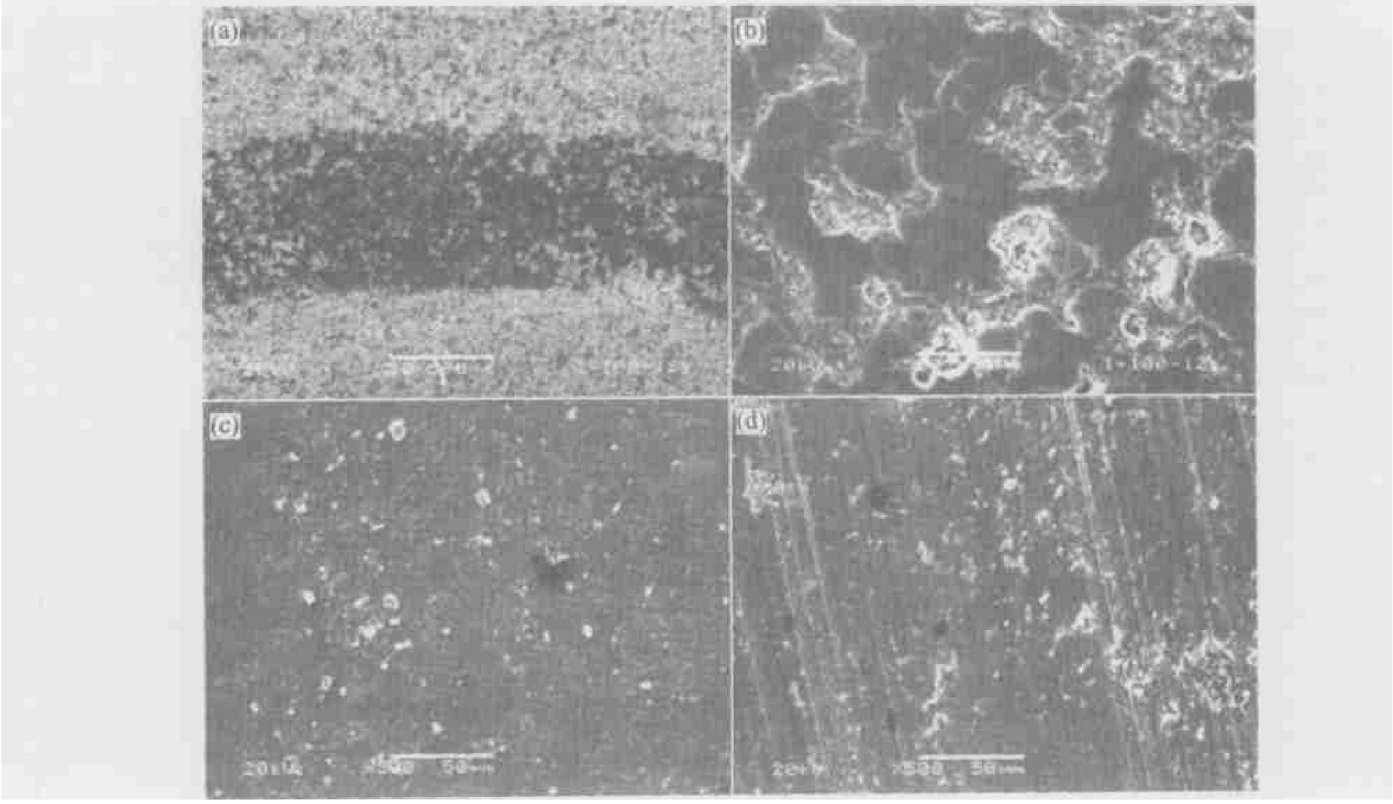

Fig. 9 SEM micrographs of worn MAO coatings and counterparts surfaces after undergoing friction tests
(a) —Worn surface of MAO coatings against Si_3N_4 ceramic ball;
(b) —Magnified picture of (a);
(c), (d) —Worn surfaces of Si_3N_4 ceramic ball and GCr15 ball, respectively

on the oxide coatings. However, not only 60 μm-thick but also 130 μm-thick oxide coatings have not been stripped from the substrate. That indicated the MAO coatings have good toughness and strong adhesion with aluminum alloy substrate. The microarc oxidation coatings have greatly improved the antiwear properties of Al alloy, but have high friction coefficient which changes in the scope of 0.7 - 0.8. Under grease lubricating, friction coefficient is only 0.15 and wear loss rate is less than 1/10 of the loss rate under dry friction. Since the microarc oxidation coatings show high hardness, excellent interfacial adhesion and mechanical properties, they could find promising application in situations where light mass and corrosion resistance are required.

Acknowledgments

We would like to thank Professor LI Bo in Lanzhou University for assisting in the tensile tests.

REFERENCES

[1] Krysmann W, Kurze P, Dittrich K H, et al. Process characteristics and parameters of anodic oxidation by spark discharge(ANOF)[J]. Crys Res Technol, 1984, 19(7): 973 - 979.

[2] Xue W B, Deng Z W, Yong Y C. The technique of microarc oxidation on aluminium alloys [J]. The Chinese Journal of Nonferrous Metals, 1997, 7(10): 140 - 143. (in Chinese)

[3] Liu J P, Kuang Y F. Microarc anodization technique and its development [J]. Materials Review, 1998, 12(5): 27 - 29. (in Chinese)

[4] Yerokhin A L, Nie X, Leyland A, et al. Characterisation of oxide films produced by plasma electrolytic oxidation of a Ti-6Al-4V alloy [J]. Surf Coat Technol, 2000, 130: 195 - 206.

[5] Wirtz G P, Brown S D, Kriven W M. Ceramic coatings by anodic spark deposition [J]. Mater Manuf Process, 1991, 6(1): 87 - 115.

[6] Tian J, Luo Z Z, Qi S K, et al. Structure and antiwear behavior of micro-arc oxidized coatings on aluminum alloy [J]. Surf Coat Technol, 2002, 154: 1 - 7.

[7] Dearnley P A, Gunnersbach J, Weiss H, et al. The sliding wear resistance and frictional characteristics of surface modified aluminium alloys under extreme pressure [J]. Wear, 1999, 225 - 229: 127 - 134.

[8] Nie X, Leyland A, Song H W, et al. Thickness effects on the mechanical properties of microarc discharge oxide coatings on aluminium alloys [J]. Surf Coat Technol, 1999, 116 - 119: 1055 - 1060.

[9] Gnedenkov S V, Khrisanfova O A, Zavidnaya A G, et al. Production of hard and heat-resistant coatings on aluminium using a plasma micro-discharge [J]. Surf Coat Technol, 2000, 123: 24 - 28.

[10] Nie X, Meletis E I, Jiang J C, et al. Abrasive wear corrosion properties and TEM analysis of Al_2O_3 coatings fabricated using plasma electrolysis [J]. Surf Coat Technol, 2002, 149: 245 - 251.

[11] Krishna L R, Somaraju K R C, Sundararajan G. The tribological performance of ultra-hard ceramic composite coatings obtained through microarc oxidation [J]. Surf Coat Technol, 2003, 163 - 164: 484 - 490.

[12] Rudnev V S, Yarovaya T P, Boguta D L, et al. Anodic spark deposition of P, Me(Ⅱ) or Me(Ⅲ) containing coatings on aluminium and titanium alloys in electrolytes with polyphosphate complexes [J]. Journal of Electroanalytical Chemistry, 2001, 497: 150 - 158.

[13] Miller W S, Zhuang L, Bottema J, et al. Recent development in aluminium alloys for the automotive industry [J]. Mater Sci Eng A, 2000, 280: 37 - 49.

[14] Heinz A, Haszler A, Keidel C, et al. Recent development in aluminium alloys for aerospace applications [J]. Mater Sci Eng A, 2000, 280: 102 - 107.

[15] Xue W B, Deng Z W, Chen R Y, et al. Growth regularity of ceramic coatings formed by microarc oxidation on Al-Cu-Mg alloy [J]. Thin Solid Films, 2000, 372: 114 - 117.

[16] Xue W B, Deng Z W, Chen R Y, et al. Microstructure and properties of ceramic coatings produced on 2024 aluminium alloy by microarc oxidation [J]. Journal of Materials Science, 2001, 36: 2615 - 2619.

(Edited by LONG Huai-zhong)